

## The oxidative potential of nanomaterials: an optimized high-throughput protocol and interlaboratory comparison for the ferric reducing ability of serum (FRAS) assay

Nienke Ruijter, Matthew Boyles, Hedwig Braakhuis, Rafael Ayerbe Algaba, Morgan Lofty, Veronica di Battista, Wendel Wohlleben, Flemming R. Cassee & Ana Candalija

To cite this article: Nienke Ruijter, Matthew Boyles, Hedwig Braakhuis, Rafael Ayerbe Algaba, Morgan Lofty, Veronica di Battista, Wendel Wohlleben, Flemming R. Cassee & Ana Candalija (2024) The oxidative potential of nanomaterials: an optimized high-throughput protocol and interlaboratory comparison for the ferric reducing ability of serum (FRAS) assay, *Nanotoxicology*, 18:8, 724-738, DOI: [10.1080/17435390.2024.2438116](https://doi.org/10.1080/17435390.2024.2438116)

To link to this article: <https://doi.org/10.1080/17435390.2024.2438116>



© 2024 The Author(s). Published by Informa UK Limited, trading as Taylor & Francis Group



[View supplementary material](#)



Published online: 14 Dec 2024.



[Submit your article to this journal](#)



Article views: 13



[View related articles](#)



[View Crossmark data](#)

# The oxidative potential of nanomaterials: an optimized high-throughput protocol and interlaboratory comparison for the ferric reducing ability of serum (FRAS) assay

Nienke Ruijter<sup>a</sup>, Matthew Boyles<sup>b,c</sup>, Hedwig Braakhuis<sup>a,d</sup>, Rafael Ayerbe Algaba<sup>e</sup>, Morgan Lofty<sup>b</sup>, Veronica di Battista<sup>f</sup>, Wendel Wohlleben<sup>f</sup>, Flemming R. Cassee<sup>a,g</sup> and Ana Candalija<sup>e</sup>

<sup>a</sup>National Institute for Public Health & the Environment (RIVM), Bilthoven, The Netherlands; <sup>b</sup>Institute of Occupational Medicine (IOM), Edinburgh, UK; <sup>c</sup>Centre for Biomedicine and Global Health, School of Applied Sciences, Edinburgh Napier University, Edinburgh, UK; <sup>d</sup>TNO Risk Analysis for Prevention, Innovation and Development, Utrecht, The Netherlands; <sup>e</sup>Leitat Technological Centre, Barcelona, Spain; <sup>f</sup>BASF SE, Ludwigshafen, Germany; <sup>g</sup>Institute for Risk Assessment Sciences (IRAS), Utrecht University, Utrecht, The Netherlands

## ABSTRACT

Successful implementation of Safe and Sustainable by Design (SSbD) and grouping approaches requires simple, reliable, and cost-effective assays to facilitate hazard screening at early stages of product development. Especially for nanomaterials (NMs), which exist in many different forms, efficient hazard screening is of utmost importance. Oxidative potential (OP), which is the ability of a substance to induce reactive oxygen species (ROS), is an important indicator of the potential to induce oxidative damage and oxidative stress. A frequently used assay to measure OP of NMs is the ferric reducing ability of serum (FRAS) assay. Although the widely used cuvette-based FRAS protocol is considered a robust assay, its low throughput makes the screening of multiple materials challenging. Here, we adapt the original cuvette-based FRAS assay protocol, into a 96-well format and thereby improve its user-friendliness, simplicity, and screening capacity. The adapted protocol allows for the screening of multiple NMs per plate, and multiple plates per day, where the original protocol allows for the screening of one NM dose-range per day. When comparing the two protocols, the adapted protocol showed slightly decreased assay precision as compared to the original protocol. The results obtained with the adapted protocol were compared using eight reference NMs in an interlaboratory study and showed acceptably low intra- and interlaboratory variation. We conclude that the adapted FRAS assay protocol is suitable to be used for hazard screening to facilitate SSbD and grouping approaches.

## ARTICLE HISTORY

Received 27 August 2024  
Revised 29 October 2024  
Accepted 26 November 2024

## KEYWORDS

FRAS; nanomaterials; ROS; SSbD; oxidative potential


## Introduction

The number and variety of nanomaterials (NMs) on the market is increasing through the manipulation of parameters such as size, shape, or the application of coatings. The large amount and quick development of new NMs requires rapid pre-market hazard screening at the early stages of product innovation. This together with the goals outlined in the European Green Deal and Chemicals Strategy for Sustainability (CSS) regarding a toxic-free environment and reducing harmful substances (EC 2019, EC 2020), has created a need for novel approaches such as Safe and Sustainable by Design (SSbD),

grouping, and read-across, which facilitate efficient risk assessment and flagging of potentially harmful NMs. These approaches in many cases rely on simple *in vitro* screening assays (Braakhuis et al. 2021, Ruijter et al. 2023). For NMs specifically, such testing methods need additional optimizations to overcome interferences and other material behaviors that complicate testing (Guadagnini et al. 2015, Gulumian and Cassee 2021).

The induction of oxidative stress (OS) is a widely accepted mechanism of action upon exposure to NMs, which is associated with adverse outcomes such as inflammation and oxidative damage to e.g. DNA (Nel et al. 2006, Ayres et al. 2008, Møller et al.

**CONTACT** Flemming R. Cassee  [flemming.cassee@rivm.nl](mailto:flemming.cassee@rivm.nl)  National Institute for Public Health & the Environment (RIVM), 3721 MA Bilthoven, The Netherlands

 Supplemental data for this article can be accessed online at <https://doi.org/10.1080/17435390.2024.2438116>.

© 2024 The Author(s). Published by Informa UK Limited, trading as Taylor & Francis Group

This is an Open Access article distributed under the terms of the Creative Commons Attribution-NonCommercial-NoDerivatives License (<http://creativecommons.org/licenses/by-nc-nd/4.0/>), which permits non-commercial re-use, distribution, and reproduction in any medium, provided the original work is properly cited, and is not altered, transformed, or built upon in any way. The terms on which this article has been published allow the posting of the Accepted Manuscript in a repository by the author(s) or with their consent.

2010, Møller et al. 2014, Song et al. 2016). OS can be induced by the oxidative potential (OP) of a NM, which is described as the ability of a NM to form potentially toxic reactive oxygen species (ROS) such as superoxide ( $O_2^-$ ), singlet oxygen ( $^1O_2$ ), and hydroxyl ( $\cdot OH$ ) radicals, or reactive nitrogen species (RNS) in their direct surroundings through redox reactions. OP and OS are part of many NM-specific hazard assessment strategies and grouping and read-across approaches due to their potential as predictors of toxicity (Arts et al. 2015, Dekkers et al. 2020, Braakhuis et al. 2021, Di Cristo et al. 2021, Janer, Landsiedel, and Wohlleben 2021).

*In vitro* acellular assays to determine OP and cellular assays to predict possible OS and oxidative damage have extensively been reviewed previously (Ayres et al. 2008, Hellack et al. 2017). Acellular assays purely measure the physicochemical property OP, whereas cellular assays account for the fact that cells can resolve ROS and for the fact that OS can be induced through other pathways besides OP (Hellack et al. 2017). Acellular assays are typically based on the detection of consumption or oxidation of chemical reagents with ROS affinity (e.g. dithiothreitol (DTT) and ascorbic acid), fluorescent probes (e.g. dichloro-dihydro-fluorescein (DCFH) assay, see Boyles et al. (2022) for nano-specific protocol), spin traps (electron paramagnetic resonance (EPR), see ISO (2017) for nano-specific protocol), or interaction with biomolecules (e.g. lipid peroxidation). In general, cellular assays for OS show a higher prediction accuracy for *in vivo* adverse outcomes as compared to acellular OP assays, and a combination of both was shown to perform even better (Riebeling et al. 2016, Hellack et al. 2017, Bahl et al. 2020). For NM hazard screening purposes for an SSbD approach, acellular OP assays may serve as a good starting point, especially when used in a high-throughput screening format. In this paper, we optimize the acellular ferric ( $Fe^{3+}$ ) reducing ability of serum (FRAS) assay for improved user-friendliness and high-throughput screening.

The FRAS method was originally developed to measure the ferric reducing ability of blood plasma (FRAP) of clinical samples in order to map anti-oxidative defenses in patients with different pathological states (Benzie and Strain 1996). The FRAP assay principle was then adapted by Rogers et al. (2008) to detect the residual antioxidant capacity of human blood serum (HBS) after incubation with NMs. Serum was used instead of plasma to avoid interference of coagulants, and the assay is now called the ferric reducing ability of serum (FRAS) assay. Further alterations were made for testing NMs specifically by optimizing incubations

times of NMs in HBS, NM mass concentrations, and centrifugation steps to remove NMs after incubation with HBS (Rogers et al. 2008). A first detailed and optimized standard operating procedure (SOP) was published by Gandon et al. (2017) and has been widely used since (Bahl et al. 2020, Achawi et al. 2021, Ag Seleci et al. 2022). In the Gandon et al. (2017) SOP, optimized incubation times, centrifugation steps and HBS-reagent ratios are used.

The FRAS assay is generally regarded as an accurate assay, with good reproducibility between runs (Rogers et al. 2008, Gandon et al. 2017). The assay is especially useful for screening of potential hazards in the context of SSbD because it can provide a more generic image of OP, as a cocktail of anti-oxidants are present in HBS, of which ascorbic acid and uric acid are most abundant (Benzie and Strain 1996). The FRAS assay has been shown to be better capable of predicting *in vitro* cellular OS as compared to the acellular DCFH assay, and was sensitive enough to distinguish the OP between different types of carbon nanotubes (CNTs) (Pal et al. 2014). Additionally, the FRAS assay outperformed EPR in predicting *in vivo* adverse outcomes from short term inhalation studies (STIS) in which a range of histopathological and bronchoalveolar lavage fluid (BALF) markers were assessed (Bahl et al. 2020). In the latter study the prediction accuracy of the FRAS assay was determined to be 50%, which is acceptable given the fact that not all adverse outcomes are due to ROS formation, and that not all ROS formation leads to adverse outcomes (Bahl et al. 2020). Altogether, the FRAS assay is a useful tool in pre-market hazard screening, and has often been a suggested assay in testing strategies for SSbD and grouping approaches (Arts et al. 2015, Dekkers et al. 2016, Braakhuis et al. 2021, Janer, Landsiedel, and Wohlleben 2021). However, the latest and most frequently used SOP of the FRAS assay as described in Gandon et al. (2017) has a relatively low throughput due to the requirement of glassware material and disposables, quartz cuvettes, and in general time-consuming procedures allowing to test only one NM dose-range per day.

Therefore, in this research the original cuvette-based SOP was adapted for high-throughput testing, maintaining its advantages as described above. The main changes that were made to the protocol were allowing the use of plastic disposables and the use of 96-well plates instead of quartz cuvettes for incubations and absorbance measurements, allowing for the testing of multiple NMs per plate and multiple plates per day. Assay robustness of the adapted protocol was assessed based on interlaboratory

comparisons of assay outcomes, and assay repeatability/precision was assessed based on intra-laboratory comparisons (Pedersen and Fant 2018). Intra- and interlaboratory reproducibility are expressed as coefficients of variation (CV), for which no guidelines exist. In literature, a threshold of 30% was used in an OECD validation study using zebrafish (Busquet et al. 2014), and in an interlaboratory study using cells (Piret et al. 2017). Since the FRAS assay does not involve cells or organisms, reproducibility was considered adequate when the coefficient of variation (CV) was below 20% in this study.

## Methods

### Experimental design

First, the original protocol (Gandon et al. 2017) was adapted to increase its throughput and user-friendliness. The newly introduced aspects such as the use of plastic disposables and the use of 96-well plates were verified in several experiments. Then, three laboratories (reference lab, lab 2 and lab 3) collaborated to compare the original and the adapted protocol to each other using dose-ranges of five NMs. Then, three laboratories (labs 1, 2, and 3) carried out an interlaboratory evaluation using eight NMs, tested at one surface area-based dose (1 m<sup>2</sup>/L) and a mass-based dose range (0-40 mg/mL).

NMs, HBS and reagents were not distributed between laboratories, and each laboratory used their own stock and equipment or ordered their own supplies. Weighing procedures (e.g. the use of a glove box or electrostatic charges neutralizer) were not harmonized. The SOP was distributed to the 3 laboratories, but no common training was provided to the people performing the assay. The participating laboratories were research laboratories and not ISO/CEN certified.

### Nanomaterials

The NMs that were used are listed in Table 1.

### Chemicals

The chemicals and reagents that were used are listed in (Table 2).

### Equipment

The equipment used in the laboratories participating in the interlaboratory study are listed in (Table 3). The laboratory that produced the original protocol (Gandon et al. 2017) provided data for the comparison of the original to adapted protocol, but did not participate in the interlaboratory study of the

**Table 1.** Nanomaterials used in this paper.

NM core composition	Supplier/Distributor	Product/NM number	Primary particle size (nm)	BET surface area (m <sup>2</sup> /g)	Reference for BET
CuO	PlasmaChem	YF131107	24	34	(Bahl et al. 2020)
CuO	Sigma Aldrich	544868	50	29	Sigma Aldrich
Ag	Sigma Aldrich	576832	<100	5	Sigma Aldrich
Ag	HeiQ RAS GmbH	5404/NM300K	<20	38.1	JRC repository
Mn <sub>2</sub> O <sub>3</sub>	Skyspring	4910DX	36	20	(Ag Seleci et al. 2022)
Mn <sub>2</sub> O <sub>3</sub>	Sigma Aldrich	463701	Unknown (non-nano)	Unknown	
SiO <sub>2</sub>	JRC Nanomaterials Repository, Ispra, Italy	NM-203	73.61	203.92	JRC repository
BaSO <sub>4</sub>	JRC Nanomaterials Repository, Ispra, Italy	BaSO4-NM220-JRCNM50001	31.5	33	PATROLS D1.1
TiO <sub>2</sub>	JRC Nanomaterials Repository, Ispra, Italy	NM105-JRCNM01005a	15-24	46	JRC repository
ZnO	JRC Nanomaterials Repository, Ispra, Italy	NM-110	42	12	(Bahl et al. 2020)

**Table 2.** Chemicals used in this paper.

Reagent/chemical name	Supplier	Product number	CAS number
Sodium acetate trihydrate BioUltra, ≥99.5%	Sigma Aldrich	71188	6131-90-4
Acetic acid, glacial, ACS, 99.7+%	Alfa Aesar	36289.AP	64-19-7
2,4,6-Tris(2-pyridyl)-s-triazine for spectrophotometric det. (of Fe), ≥98%	Supelco	T1253	3682-35-7
Iron (III) chloride hexahydrate puriss. p.a., ACS reagent, crystallized, 98.0-102% (RT)	Sigma Aldrich	44944	10025-77-1
Human Serum from platelet poor human plasma, sterile-filtered (mycoplasma tested, virus tested)	Sigma Aldrich	P2918-100ml	NA
(±)-6-Hydroxy-2,5,7,8-tetramethylchromane-2-carboxylic acid (Trolox)	Sigma Aldrich	238813-5G	53188-07-1
1 M Hydrochloric acid (HCl)	Riedel-De Haen*	7647-01-0	7647-01-0

\*If the lab had a preexisting stock of HCl, this was used.

**Table 3.** Equipment used in the laboratories participating in this study.

Laboratory name	Ultrasonication bath	Spectrophotometer	HBS	Microbalance
Lab 1	Selecta ULTRASON-H	SYNERGY – BioTek	Sigma P2918	Mettler Toledo Excellence, XS205DU
Lab 2	Elmasonic S100	Spectramax M2	Sigma P2918	Sartorius MSE 125 P-1000D1
Lab 3	VWR USC-T Ultrasonic bath	Tecan Infinite M Plex	Sigma P2918	SLS Lab Pro SR-150AZ
Reference Lab	Bandelin Sonorex Digiplus DL 156 BH	PerkinElmer Lambda 35	Sigma P2918	Mettler Toledo XPE 205

adapted protocol. This laboratory is referred to as Reference Lab throughout the manuscript.

### **Original Cuvette-based FRAS protocol**

In the FRAS assay, the decrease of antioxidants in HBS after exposure to NMs is quantified. The exact SOP as published in Gandon et al. (2017) was followed. In short, NMs were weighed in glass vials (0, 1.13, 3, 8.25, 22.5, and 60 mg), after which exactly 1.5 mg HBS was weighed to the same vials to achieve concentrations 0, 0.75, 2, 5.5, 15, and 40 mg/mL. The vials were sonicated for 1 min using bath sonication with maximum power at room temperature and incubated for 3h at 37°C whilst stirring. The mixture was centrifuged 2.5h at 14000 x g to remove NMs, after which 100 µl of supernatant was transferred to clean glass vials containing 2 grams of FRAS reagent consisting of ferric ions (Fe<sup>3+</sup>) and 4,6-tripyridyl-s-triazine (TPTZ) in acetate buffer. The remaining antioxidants in the HBS reduce Fe<sup>3+</sup> to Fe<sup>2+</sup> forming a Fe<sup>2+</sup>-TPTZ complex with a bright blue color. The mixtures were incubated for exactly 1h in the dark whilst shaking. The antioxidant capacity of HBS was then determined by transferring the mixtures to quartz cuvettes and measuring absorbance at 593nm using a spectrophotometer. Only glass materials and disposables were used. All pipetting steps were carried out using transferpettor pipettes with glass capillary tips. For an overview of the SOP, see Figure 1.

### **Original Cuvette-based protocol with plastic disposables**

As a first optimization step the original FRAS protocol published in Gandon et al. (2017) was adapted for the use of plasticware material instead of glassware. The critical HBS-NM incubation step was still carried out in glass vials; however, the vials were agitated during incubation instead of stirred to improve assay accessibility and throughput. Briefly, NMs were weighed in glass vials (0, 1.13, 3, 8.25, 22.5, and 60 mg), after which ±1.5 mL of HBS was added using a micropipette and plastic tips, instead of weighing, to achieve the exact concentrations 0,

0.75, 2, 5.5, 15, and 40 mg/mL. Samples were sonicated in an ultrasonicator bath for 1 min with maximum power at room temperature and incubated for 3h in the dark at 37°C with agitation at 150rpm. Afterwards, samples were transferred to plastic ultracentrifuge tubes using plastic pipette tips and centrifuged using an ultracentrifuge for 2.5h at 14000 x g. FRAS reagents and the Trolox standard curve were prepared following the original protocol. 2 mL of FRAS reagent was added to small glass vials using a micropipette and plastic tips, instead of weighing. 100 µL of the sample supernatant (or Trolox standard) was added to the vials containing the FRAS reagent, using a plastic tip, and incubated for 1h in the dark with agitation. Samples were transferred to plastic cuvettes with a plastic micropipette tip, and absorbance was measured at 593 nm.

### **Adapted 96-well FRAS protocol**

To adjust the FRAS assay for high-throughput screening, several adaptations were made to the original (Gandon et al. 2017) cuvette-based SOP. Only those aspects that were necessary to increase throughput and ease of use of the assay were adapted. NM doses, incubation times, relative centrifugal force (RCF), centrifugation times, and HBS/FRAS reagent ratios etc. were all unchanged. Changes made include:

- The use of 96-well plates instead of quartz cuvettes for read-outs. FRAS reagent incubations are also carried out in the same 96-well plates.
- The use of shaking instead of stirring for the NM-serum incubations. Since the throughput of the assay is increased, many magnetic stirring beads would otherwise be required.
- Use of micropipettes for pipetting all volumes, instead of weighing them.
- Allowing use of plastic equipment and disposables instead of all-glass equipment. This also includes the use of plastic pipette tips, no longer necessitating transferpettors with glass capillary tips. The use of plastic disposables greatly increases the accessibility



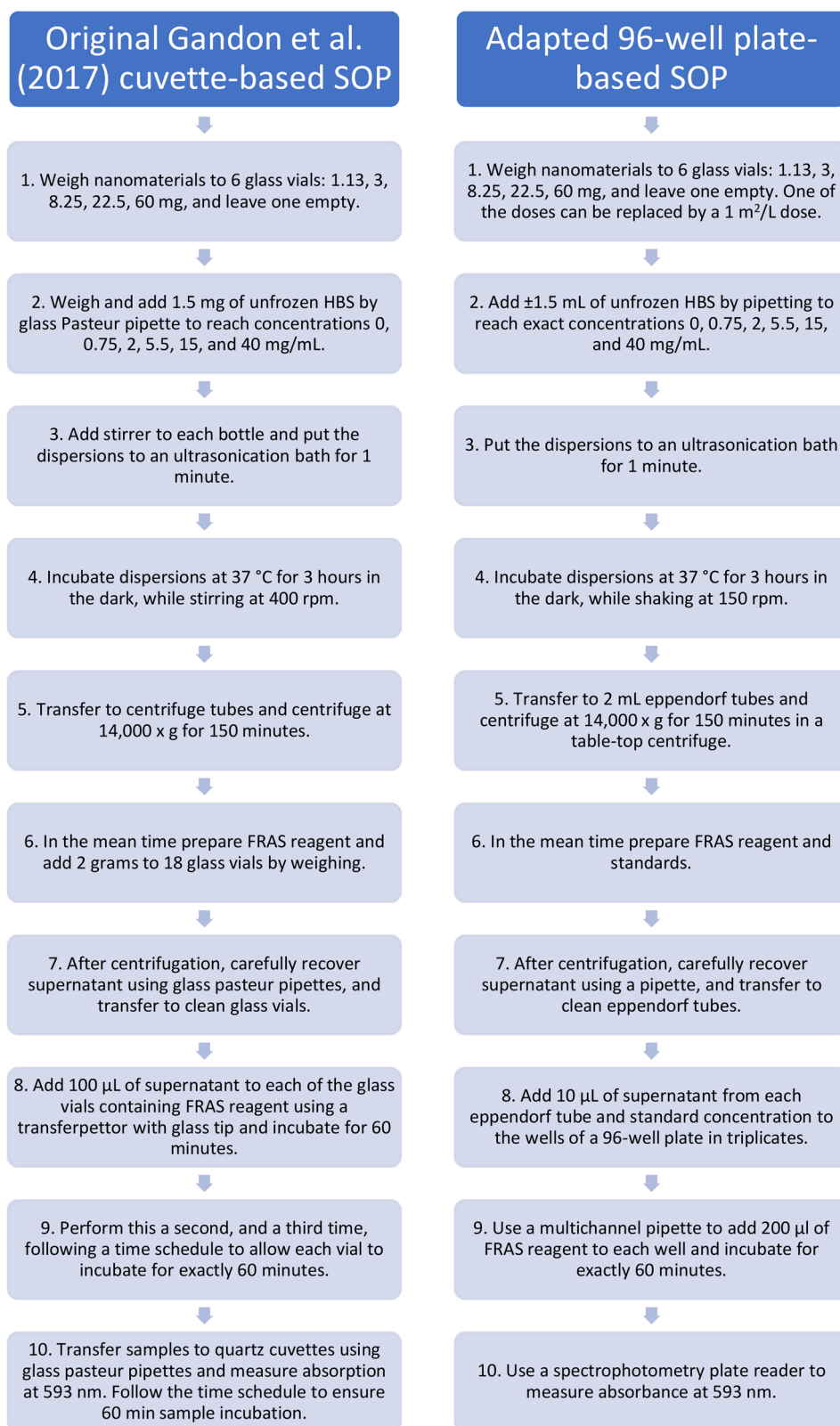


**Figure 1.** A side-by-side comparison between the original and the adapted FRAS assay protocols. The original Cuvette-based assay allows for testing of one dose-range per day. The adapted 96-well plate-based assay allows for the testing of four dose-ranges per 96-well plate, and multiple 96-well plates per day.

and feasibility of this assay. The HBS-NM incubation step is however still carried out in glass vials.

- The use of CuO NMs (Sigma) as a positive control instead of Mn<sub>2</sub>O<sub>3</sub> NMs, as the Mn<sub>2</sub>O<sub>3</sub> (4910DX) that was used in the original

protocol is no longer available at Skyspring. The CuO NMs were previously shown to have a high OP (Bahl et al. 2020).

- A slightly larger Trolox standard curve to accommodate the new assay format.

The adapted SOP can be found in [Supplemental Materials 1](#). An overview of the adapted SOP and a comparison to the original SOP are shown in [Figure 1](#).

### Data analysis

Calculations were performed as in Gandon et al. (2017) and are described in more detail below.

#### Trolox equivalent units

The Trolox (Water soluble vitamin E analogue) standard curve is used to calculate Trolox Equivalent Units (TEU, in  $\mu\text{M}$ ), which allows for the standardization of results compared to a known amount of antioxidants. TEU is calculated using the slope of the trolox standard curve. The standard curve can be fitted as:  $\text{Abs}_{\text{Trolox}} = kE * I * d * C_{\text{Trolox}} [\text{mM}] + b$ . Where:

- Abs=absorption at wavelength 593 nm.
- kE=extinction coefficient of the  $\text{Fe}^{2+}$ /TPTZ complex induced by 1 mol of antioxidants (TEU, in  $\mu\text{M}$ ).
- I=light path through cuvette/well in cm. For a well this is the height of the liquid in the well.
- d=dilution factor. In our case 0.0476 (0.1 mL of HBS and 2 mL FRAS reagent).
- c=concentration of Trolox in mM.
- b=intersection of the standard curve with the y-axis.  $kE * I * d$  is equivalent to the slope of the standard curve, meaning that TEU can be calculated as follows:

$$\text{TEU}(\mu\text{M}) = \frac{\text{Abs}_{\text{sample}}}{\text{Slope}_{\text{standard curve}}} * 1000$$

Multiplying by 1000 allows for the conversion of the Trolox concentration in mM to TEU which is expressed in  $\mu\text{M}$ .

It would be more accurate to calculate TEU based on the slope as well as the intersect of the Trolox standard curve. But previous papers have only used the slope, and not the intersect. Therefore, to be able to compare data, this approach was also

followed in this current paper. Additionally, when calculating the BOD in the next step, the subtraction of the intersect is canceled out by subtracting the two TEU values.

#### Biological oxidative damage

Biological oxidative damage (BOD) uses the TEU of the blank sample (unexposed HBS with FRAS reagent) to indicate the increase in oxidative damage to the HBS sample due to the NM incubation. The BOD is calculated as follows:

$$\text{BOD}(\mu\text{MTEU}) = \text{TEU}_{\text{blank}} - \text{TEU}_{\text{sample}}$$

Or similarly as:

$$\text{BOD}(\mu\text{MTEU}) = \frac{\text{Abs}_{\text{blank}} - \text{Abs}_{\text{sample}}}{\text{Slope}_{\text{standard curve}}} * 1000$$

#### Mass specific biological oxidative damage

Mass specific BOD values (mBOD) are calculated as follows:

$$\text{mBOD}(\text{nmolTEU} / \text{mg}) = \frac{\text{BOD}(\mu\text{MTEU})}{\text{Concentration}(\text{g} / \text{L})}$$

#### Surface specific biological oxidative damage

Surface specific BOD values (sBOD) are calculated as follows:

$$\text{sBOD}(\text{nmolTEU} / \text{m}^2) = \frac{\text{BOD}(\mu\text{MTEU})}{\text{Dose}(\text{m}^2 / \text{L})}$$

Where:

$$\text{Dose}(\text{m}^2 / \text{L}) = \text{Concentration}(\text{g} / \text{L}) * \text{BET}(\text{m}^2 / \text{g}) / 1000$$

BET = BET surface of nanomaterial as obtained by Brunauer-Emmett-Teller method.

#### Coefficient of variation

To assess assay precision and repeatability, the coefficient of variation (CV) was calculated as follows:

$$\text{CV}(\%) = \frac{\text{Standard deviation}}{\text{Mean}} * 100$$

For this calculation, TEU values at wavelength 593 nm were used so that the variation in slope of the standard curve is also included. BOD values could not be used as they cannot be calculated for

HBS-only conditions. Independent experiment outcomes (biological replicates) and not technical replicates were used for calculating CV. Presented CVs are therefore always between-run CVs.

### Limit of detection

Limit of detection (LOD) is calculated as follows:

$$LOD(TEU(\mu M)) = 3.3 * \frac{SD \text{ of TEU of HBS control}}{\text{Slope of the standard curve}}$$

### Statistical analysis

Each individual experiment was carried out three times in each laboratory, each experiment containing three technical replicates (wells or cuvettes) originating from the same NM-exposed HBS vial. Averages of each biological replicate were analyzed by one-way ANOVA, followed by Tukey's multiple comparisons test, using GraphPad Prism version 9.5.1., unless otherwise specified.

## Results

### Verification of adaptations

To create the adapted (96-well plate-based) protocol, the changes as described in the methods sections were made to the original (cuvette-based) Gandon et al. (2017) protocol. Below, the comparison of using plastic consumables versus glassware and the use of 96-well plates versus cuvettes are shown in more detail before comparing the fully adapted protocol to the original protocol.

#### The use of plastic consumables instead of glassware

The original SOP specifically states to only use glassware (including pipette tips, incubation tubes, and cuvettes) to avoid potential interferences with plastic materials. The advantages of allowing the use of plastic disposables are: i) the centrifugation step can be carried out in a table-top centrifuge using plastic Eppendorf tubes, and ii) regular pipettes with plastic tips instead of transferpette pipettes with glass capillary tips can be used. Allowing the use of plastics therefore makes the adapted protocol accessible to more laboratories. Four NMs were tested following the original protocol but using plastic disposables instead of glass, and no differences in BOD were observed when comparing to the glass-only original protocol (Figure 2).

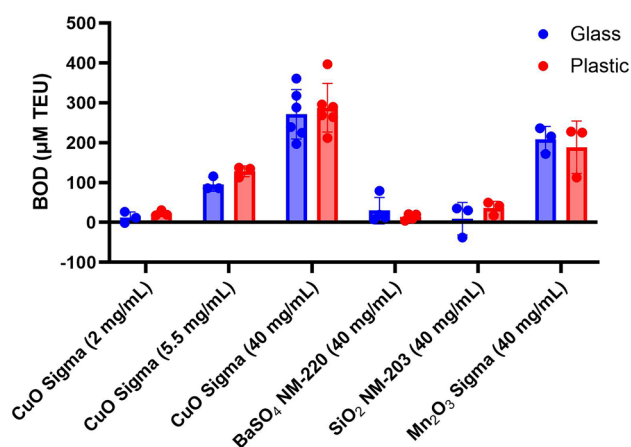


**Figure 2.** Comparison between the original FRAS protocol using glassware and the original protocol using plasticware in lab 1. BOD values of NMs using the glass protocol (blue) vs the plastic protocol (red). Data was analyzed using a t-test, and results show no significant differences between the two protocols.

#### The use of 96-well plates instead of cuvettes for incubations and spectrophotometric readout

Changing from a cuvette- to a 96 well-based format required a 10-fold reduction in reaction mixture volume. It was confirmed that the HBS to FRAS reagent ratio that was used in the original protocol was still appropriate in the new format for both the standard curve as well as for a positive control by testing a range of ratios (Figure S1). The linear range of the standard curve was determined as well and was found to be larger than the linear range of the cuvette-based protocol (0.001-0.5 mg/mL Trolox vs 0.001-0.1 mg/mL Trolox for the original protocol, shown in Figures S2 and S3).

#### Comparison between original and adapted protocol

A direct comparison between the original and the adapted protocol within the same laboratory (lab 2) using positive control CuO NMs (Sigma) is shown in Figure 3. Each line represents one independent experiment of each protocol. TEU values are similar using both protocols (Figure 3B), but because the baseline TEU of HBS is higher in the adapted as compared to the original protocol, the resulting BODs of the two protocols do not align (average 2.2 fold higher in adapted protocol as compared to original at the 5.5, 15, and 40 mg/mL doses) (Figure 3C). Table 4 shows intra-laboratory CVs using TEU values, as absorbance values do not take into account the variation in the slope of the standard curve and BOD values require subtraction of HBS



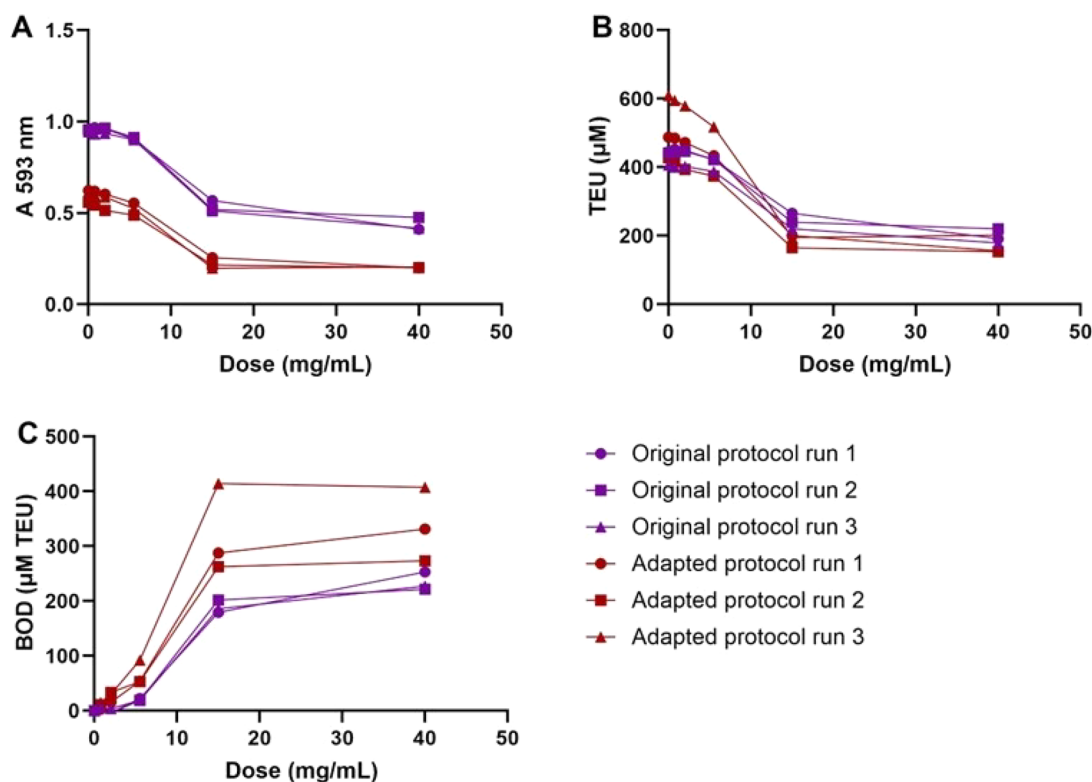


**Figure 3.** Comparison between the original Gandon et al. (2017) and adapted (96-well plate-based) protocols for CuO (Sigma) NMs in lab 2. Each point represents the average of three technical replicates in one independent experiment, and therefore error bars are not shown. Results are expressed as: Absorbance values at 593 nm (A); Trolox equivalent Units ( $\mu\text{M}$ ) (B); and biological oxidative damage ( $\mu\text{M TEU}$ ) (C).

**Table 4.** Intra-laboratory variability expressed as coefficients of variance (CV) based on TEU values in the two protocols when testing CuO (Sigma) NMs in lab 2.

	CV using original protocol (%) (n=3)	CV using adapted protocol (%) (n=3)
HBS	4.95	18.27
0.75 mg/mL	6.40	18.11
2 mg/mL	6.01	19.34
5.5 mg/mL	4.90	16.27
15 mg/mL	9.39	10.06
40 mg/mL	10.65	16.03

n = number of independent experiments.

TEU values and can therefore not be calculated for HBS-only conditions. TEU values are reproducible within the original as well as within the adapted protocol, with a better precision when following the original protocol (Table 4). The third run with the adapted protocol has an exceptionally high BOD throughout the dose-range (Figure 3B), which seems to have been caused by a slightly different slope of the Trolox standard curve. This is also reflected in CV values reported for the adapted protocol in Table 4.

The comparison between BOD values using the original and adapted protocol using four additional NMs in three different laboratories

(including the reference lab) is shown in Figure 4. Corresponding absolute absorbance and TEU values from these experiments are shown in Figure S4. BOD values resulting from the original and adapted protocol follow the same trends, indicating that the assay sensitivity is not lost due to the adaptations for high throughput. BOD values are generally lower when using the original protocol, and fewer outliers are observed when using the original protocol.

The quality of the Trolox standard curve and the HBS-only condition are partially indicative of the assay's performance. A visual comparison between the standard curves of the two protocols can be found in Figure S5. Table 5 shows relevant parameters of the two protocols when testing HBS alone and Trolox standard curves in lab 2 and in the reference lab. Linear correlation coefficients ( $R^2$ ) of both protocols are good (0.999 using both SOPs), and the linear range of the standard curve is improved in the adapted protocol, as described earlier. The TEU of HBS (of the same batch) is comparable enough between protocols (435.42  $\mu\text{M TEU}$  in the original protocol and 466.10  $\mu\text{M TEU}$  in the adapted protocol). The reference laboratory used a

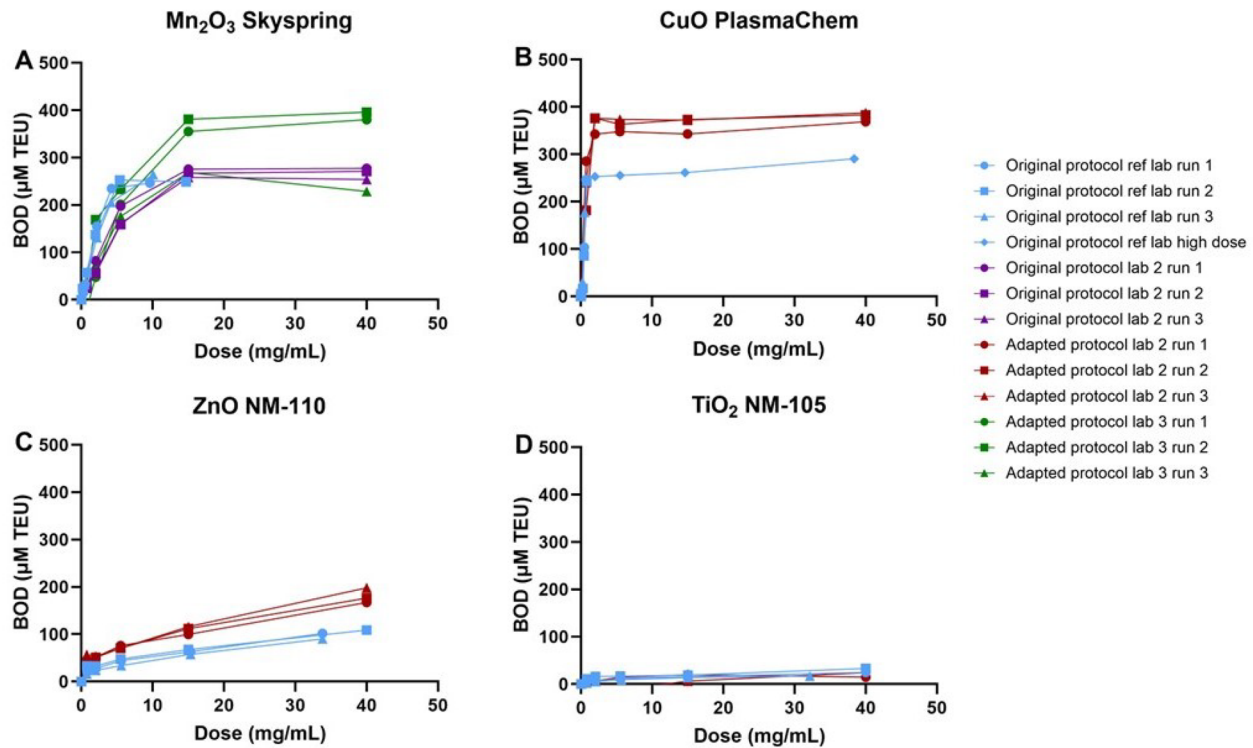


**Figure 4.** Comparison of the biological oxidative damage (BOD) values of four nanomaterials obtained with the original and adapted FRAS protocols. Results are expressed as BOD ( $\mu\text{M TEU}$ ). Each line represents the average of three technical replicates in one independent experiment, and therefore error bars are not shown. Comparisons were not carried out within the same laboratory due to practical considerations.

**Table 5.** Comparison of parameters of the standard curve and HBS-only measurements using the original and adapted protocols, carried out in lab 2 and in the reference lab.

	Original protocol in reference lab (n=6)		Original protocol in lab 2 (n=6)		Adapted protocol in lab 2 (n=6)	
	Average	SD	Average	SD	Average	SD
Slope of standard curve (a)	2.654	0.040	2.168	0.079	1.166	0.049
Intersect of standard curve (b)	0.075	0.009	0.083	0.005	0.063	0.006
R <sup>2</sup> of standard curve	0.999	0.001	0.999	0.002	0.999	0.001
Absorption HBS (593 nm)	0.970	0.024	0.943	0.017	0.583	0.032
TEU of HBS ( $\mu\text{M}$ )	364.68	11.00	435.42	15.88	466.10	26.42
Dilution factor (d)	0.048		0.048		0.048	
Light path (l) (cm)	1.0		1.0		1.313	
Extinction coefficient (kE)	55.76	0.50	45.52	1.66	20.02	0.78
Linear range of standard curve	0.001-0.1 mg/mL Trolox		0.001-0.1 mg/mL Trolox		0.001-0.5 mg/mL Trolox	
Limit of Detection (TEU value)	13.68		24.17		74.73	

n = number of independent experiments.

different batch of serum and can therefore not be compared in the TEU metrics. BOD metrics correct for differences in baseline serum antioxidant capacity, which is why TEU values are not used to report FRAS assay results. Most standard deviations (SDs) are lower when using the original protocol, highlighting an enhanced precision when incubating and measuring absorbance following the original protocol. Additionally, SDs in the reference lab are lower as compared to lab 2 when using the original protocol, pointing to enhanced precision after extensive training and use of the protocol. As a

result, the limit of detection (lowest TEU value accurately detected) is lowest in the reference lab ( $13.68 \mu\text{M TEU}$ ), slightly higher in lab 2 using the original protocol ( $24.17 \mu\text{M TEU}$ ), and highest using the adapted protocol ( $74.73 \mu\text{M TEU}$ ).

### Interlaboratory comparison

The adapted protocol was evaluated in an interlaboratory study comprising of three independent laboratories using eight NMs. Biological oxidative damage measured using the adapted FRAS assay

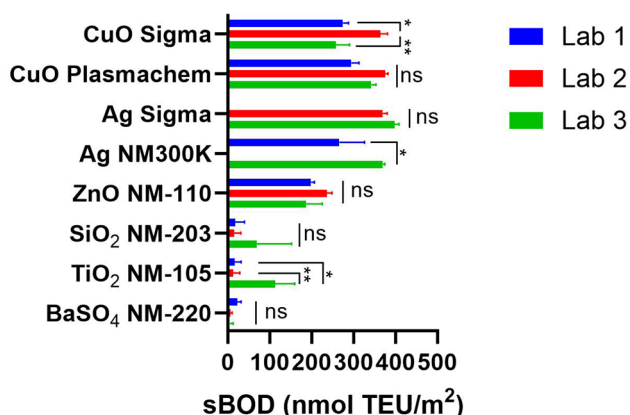


**Figure 5.** Interlaboratory comparison of the adapted (96-well plate-based) FRAS assay protocol. Results are expressed as surface based biological oxidative damage (sBOD), and doses used are 1 m<sup>2</sup>/L. Since the dose is 1 m<sup>2</sup>/L, the resulting sBOD values are the same as BOD values. Each laboratory carried out three independent experiments with each three technical replicates. Not all particles were tested in all laboratories due to practical reasons. \* p < 0.05; \*\* p < 0.01 using one-way ANOVA. ns = not significant.

in the different laboratories were compared at the surface-area adjusted dose of 1 m<sup>2</sup>/L. **Figure 5** shows good reproducibility of the adapted protocol across laboratories. CuO NMs (Sigma) showed a larger sBOD in lab 2 (364.1 ± 16.8 versus 274.8 ± 12.9 and 257.6 ± 32.8 in labs 1 and 3 respectively), NM-105 showed a larger sBOD in lab 3 (112.0 ± 47.6 versus 15.7 ± 16.1 and 12.0 ± 16.2 in labs 1 and 2 respectively), and the sBOD induced by NM300K was also significantly different between lab 1 (265.9 ± 59.8) and lab 3 (369.8 ± 4.6) (not tested in lab 2). Batch-to-batch differences may explain these deviations as particles were not distributed between laboratories and each participating laboratory used or ordered their own NMs. All intra- and interlaboratory CVs are listed in **Table S1**. The average intra-laboratory CVs are 4.72 ± 2.34%, 5.17 ± 1.75%, and 14.25 ± 8.55% in laboratory 1, 2, and 3, respectively. The average interlaboratory CV for all particles tested is 12.66 ± 4.48%, which is well below the 20% cutoff value.

Mass-based dose ranges were tested for four NMs (**Figure 6**), and significant differences were only found in high-dose NM-110 and low-dose CuO conditions. The BODs are otherwise very similar between laboratories. The parameters related to the Trolox standard curve using the adapted protocol can be found in **Table S2** and are similar across laboratories. Slopes, intercepts, and R<sup>2</sup> values are similar between laboratories, and are reproducible within laboratories (low SD). The average slope between the three

laboratories of the Trolox standard curve is 1.191 (± 0.03). The TEU of HBS differs between laboratories and batches, which is due to natural batch-to-batch differences.

## Discussion

### Assay performance

To our knowledge, this is the first publication in which the FRAS assay is adapted for high-throughput screening, using 96-well plates instead of single quartz cuvettes. Using the adapted protocol, we obtained robust results with sufficiently low intra- and interlaboratory variability, with the majority of intra- and interlaboratory CVs below 20%. No major issues were expected, as this assay has been well thought-out and was optimized in several publications (Benzie and Strain 1996, Rogers et al. 2008, Gandon et al. 2017), of which the most notable one was Gandon et al. (2017). None of the critical parameters, such as incubation times, relative centrifugal force (RCF), centrifugation times, and HBS/FRAS reagent ratios were changed. Only those parameters that facilitated high-throughput screening and overall easiness of the assay were adapted.

The three institutes participating in the interlaboratory evaluation of the adapted FRAS protocol did not receive any common training other than the SOP. The fact that each partner used their own stock of reagents, NMs, and HBS, and their own equipment (e.g. weighing and sonication devices), and yet very limited variation occurred, underlines the robustness and simplicity of the adapted FRAS assay protocol.

### Standard curve and HBS-only conditions

In the interlaboratory comparison of the adapted protocol, slopes, intercepts, and R<sup>2</sup> were very consistent within and between laboratories for Trolox. The standard curve resulting from the 96-well protocol was linear up to 0.5 mg/mL Trolox (0–2 mM Trolox) and showed excellent R<sup>2</sup> coefficients in all three laboratories. The standard curve in the original protocol is linear until 0.1 mg/mL (Gandon et al. 2017), giving the adapted protocol a larger detection range, avoiding saturation of the signal at higher reactivity, which has previously been reported for the original protocol (Achawi et al. 2021).

The average slope found in this current paper using the original protocol was 2.168 in lab 2, which is similar to the 1.9625 found in Achawi et al.

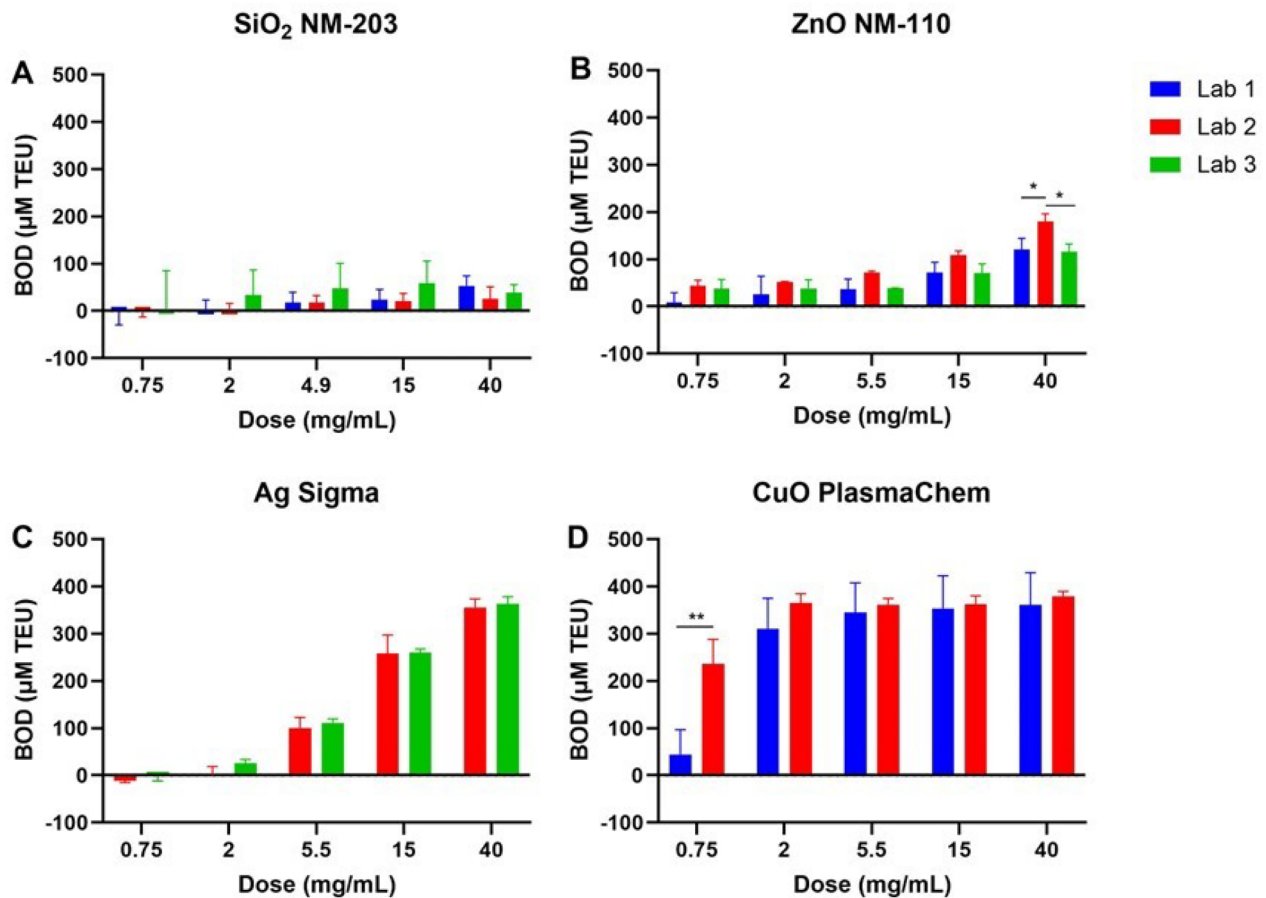


**Figure 6.** Interlaboratory comparison of mass-based dose-ranges of three different NMs across three laboratories. Results are expressed as biological oxidative damage (BOD). Each laboratory carried out three independent experiments with each three technical replicates. Not all particles were tested in all laboratories due to practical reasons. \*  $p < 0.05$ ; \*\*  $p < 0.01$  using one-way ANOVA.

(2021) using the exact same protocol. The standard curve slope in the reference lab was 2.654, which is more or less comparable. Slopes of 4.18 have been reported in papers using other cuvette-based protocols, which are not comparable to ours (Rogers et al. 2008, Hsieh et al. 2013). Using the adapted protocol, the average slope between the three laboratories was 1.191. The difference between the slopes resulting from the original and adapted protocol can be explained by detection method-related differences (cuvettes vs 96-well plates).

The extinction coefficient ( $kE$ ) of TPTZ induced by 1 Mol Trolox that was found in this paper using the original protocol in lab 2 was 45.5, which is similar to the 55.76 found in the reference lab. However, using the adapted protocol this became 20.02, which can be explained by the read-out method causing a smaller slope and longer pathway length, leading to a lower  $kE$ .

Interlaboratory differences in HBS TEU that were observed in this study can be explained by

batch-to-batch differences in antioxidants, which is also reflected by HBS TEU in other publications: 530  $\mu\text{M}$  (Hsieh et al. 2013), 366  $\mu\text{M}$  (Gandon et al. 2017), and 526  $\mu\text{M}$  (Rogers et al. 2008). Reporting FRAS assay results as BOD corrects for batch-to-batch differences in HBS antioxidants.

#### NM-treated conditions

Comparisons to literature were initially difficult for NM-treated conditions, as exact BOD, mBOD, sBOD or TEU values were scarcely reported. The authors of Gandon et al. (2017), Bahl et al. (2020), and Ag Seleci et al. (2022) kindly provided the data used for their manuscripts, which were included in the current paper as 'Reference Lab.'

Absorbance values of NM-treated HBS are not comparable between the original and the adapted protocol due the use of cuvettes vs 96-well plates, which is corrected for when converting absorbance to TEU values. Higher TEU values of HBS alone in

the adapted protocol result in higher BOD values for NM-treated conditions. The 2.2-fold difference in BOD between the two protocols indicates that results can probably not be compared between the two protocols. This means results obtained using the adapted protocol cannot be benchmarked against BODs obtained with the original protocol in the past. Calculating relative potency factors by comparing to the positive control BOD value, as performed Di Battista et al. (2024b) might solve this problem.

Gandon et al. (2017) reported a difference in assay outcome when using glass capillary pipette tips versus plastic tips, likely due to the sticking of assay components and NMs to the plastic. Here we show no influence of the use of plastic consumables on assay outcomes. These outcomes are based on only four NMs and should ideally be confirmed using more materials. The critical HBS-NM incubation step is still carried out in glass vials in the adapted protocol, and therefore we expected little to no effect of allowing the use of plastic disposables in the other steps.

### **Future optimizations**

Several aspects of the assay may be worth investigating and optimizing further. Firstly, it may be worth exploring shorter incubation and centrifugation steps to reduce the overall assay duration, while avoiding the potential trade off in sensitivity (by shorter incubation) and robustness (by optical interference of remaining NMs after shorter centrifugation). Both protocols (original and adapted) take approximately 8 hours as the limiting factors are the incubation and centrifugation steps. Shorter incubations of NMs with HBS and shorter centrifugation times have been implemented successfully before (Benzie and Strain 1996, Hsieh et al. 2013), but require further verification. Centrifugation times required for NMs can be calculated based on centrifugation speed, NM density and HBS density, but should be kept constant between NMs to allow for accurate comparison. Secondly, maximum storage times for the S1, S2, and S3 components of the FRAS reagent, and the Trolox solution should be determined, as making them freshly every single day can be time-consuming. Thirdly, reducing HBS volumes used in the assay from 1.5 mL to 1.0 mL will help reduce the amount of NM needed, which can be a limiting factor. Assay performance using reduced HBS volumes, keeping the same doses in mg/mL, should be explored further also due to the high cost of HBS. Finally, the assays throughput may be further increased. The adapted

protocol allows analyzing four NM dose-ranges per plate and multiple plates per day, depending on the available centrifuge slots available in the laboratory. Through the use of in-plate NM-HBS incubations and centrifugation steps the throughput of the adapted protocol could be further increased. None of the steps in the SOP are too complicated to be performed by laboratory robots, and the use of 384-well plates may also be explored. This assay has the potential for fully automated high throughput screening in an industrial setting, although ethical considerations regarding the use of large amounts of HBS should be reflected upon.

### **Problematic materials and interferences**

The extensive centrifugation step included in both SOPs ensures thorough separation of NMs from the HBS before incubating the HBS with FRAS reagent. Optical interference by the NMs themselves, or interference by NMs reacting with the FRAS reagent are therefore highly unlikely. However, some NMs may cause a discoloration of the HBS, as was seen in the current study for CuO NMs, and by Ag Seleci et al. (2022) for NM pigments. When the FRAS assay is applied to NMs of extremely low density, the currently applied centrifugal forces may not be sufficient for total separation of NMs and HBS. A filtration step may be added to the SOP to ensure complete separation, as was performed for graphene-based materials in Achawi et al. (2021).

In an acellular assay such as the FRAS assay, OP is measured as a rate of depletion of a reductor (in this case HBS antioxidants). OP assays do not measure reductor depletion by OP only since release of reactive ions by dissolution will also lead to a depletion. To assess the contribution of ions released from the NM to the reduction of HBS antioxidants in the FRAS assay, we recommend to follow the protocol by Peijnenburg et al. (2020). As the current study was focussed on interlaboratory comparisons of the adapted FRAS assay protocol, this was not performed.

### **The FRAS assay within an SSbD approach**

Owing to its robustness and simplicity, the FRAS assay has the potential to be applied in an SSbD approach in several ways. Firstly, the FRAS assay can be used to flag NMs of high concern in a hazard testing strategy for SSbD purposes, as is the approach of the SAbyNA guidance platform (Cazzagon et al., in preparation). Secondly, the FRAS assay is a valuable tool to assess OP in order to



justify grouping of sets of nanoforms (NFs) and read-across, as is the approach in the GRACIOUS integrated approaches to testing and assessment (IATA) for grouping purposes (Stone et al. 2020, Braakhuis et al. 2021), in the ECETOC NanoApp (Janer, Landsiedel, and Wohlleben 2021), and in the DF4NanoGrouping approach (Arts et al. 2015). Janer, Landsiedel, and Wohlleben (2021) suggested the threshold for similarity of two NFs specifically for the FRAS assay to be 'reactivity values within a factor of 5-fold for the two NFs under comparison.' And Arts et al. (2015) suggested the grouping of NFs as passive when reactivity was <10% of  $Mn_2O_3$  reactivity in the FRAS assay, and as active when reactivity was  $\geq 10\%$  of  $Mn_2O_3$  reactivity in the FRAS assay. In the GRACIOUS framework NFs are not grouped as passive or active but rather assessed for similarity based on NF potency in a dose-response approach (Braakhuis et al. 2021). Thirdly, the FRAS assay may help making SSbD choices by performing direct comparisons between a NM and its SSbD alternative for the same intended use, between several SSbD candidates, or between an SSbD candidate and a data-rich benchmark material, as is the approach in the HARMLESS project (Di Battista et al. 2024a, Di Battista et al. 2024b). For the above approaches it should be kept in mind that the FRAS assay measures the physico-chemical property OP and will not predict oxidative stress in all cases.

The suitability of several OP assays for SSbD applicability were previously reviewed in Ruijter et al. (2023). In this comparison, the FRAS assay was found to be more suitable as compared to the acellular DCFH assay, and equally as suitable as EPR and the hemolysis assay. The choice in assay should however depend on the research question, as the FRAS assay can screen for a very wide range of radicals, whereas EPR can provide information about specific types of radicals induced by the particles depending on the spin trap used (Ruijter et al. 2023).

Data FAIRness (Findable, Accessible, Interoperable, Reusable) is crucial for SSbD approaches (Caldeira et al. 2023), and can be achieved through the use of common data templates. The HARMLESS project has produced such a template for the FRAS assay, which can be found here: <https://zenodo.org/records/7729589>.

## Conclusion

We conclude that the adapted (96-well plate-based) FRAS assay protocol has improved user-friendliness,

simplicity, and a higher throughput as compared to the original (cuvette-based) FRAS assay protocol. Assay precision and limit of detection were slightly decreased in the adapted protocol as compared to the original protocol but were still satisfactory. In the interlaboratory evaluation we have shown that the adapted SOP scored well in terms of robustness and repeatability, with intra- and inter-laboratory coefficients of variation generally below 20%. The adapted FRAS assay protocol has the potential to be used for high-throughput screening purposes, which is highly needed for approaches such as SSbD.

## Acknowledgments

The authors would like to thank Fiona Murphy and Pawel Pokorski from Herriot-Watt University, and Edwin Zwart from the Centre for Health Protection at the RIVM for testing previous versions of the adapted protocol and providing their input for optimizations. The authors would also like to thank Wanda van der Stel from the Centre for Sustainability, Environment and Health at the RIVM for critically reviewing the manuscript.

## Authors' contributions

NR developed methodology, coordinated interlaboratory study, carried out experiments and wrote manuscript. MB developed methodology, carried out experiments and reviewed manuscript. HB supervised project and reviewed manuscript. RAA developed methodology and carried out experiments. ML carried out experiments and reviewed manuscript. VB and WW provided existing data as reference lab and reviewed manuscript. FRC supervised project and reviewed manuscript. AC developed methodology, coordinated interlaboratory study, carried out experiments and reviewed manuscript.

## Disclosure statement

Veronica di Battista and Wendel Wohlleben are employees of BASF SE, a company marketing nanomaterials.

## Funding

This research was funded by the SAbyNA project, European Union's Horizon 2020 research and innovation program under grant agreement No 862419, by the Dutch Ministry of Infrastructure and Water Management, and by European Union's Horizon 2020 Research and Innovation Programme under grant agreement no. 953183 (HARMLESS).

## Data availability statement

The SAbyNA project data will be publicly available in the eNanoMapper database from the 1<sup>st</sup> of June 2025.

## References

- Achawi, S., B. Feneon, J. Pourchez, and V. Forest. 2021. "Assessing Biological Oxidative Damage Induced by Graphene-Based Materials: An Asset for Grouping Approaches Using the FRAS Assay." *Regulatory Toxicology and Pharmacology: RTP* 127: 105067. <https://doi.org/10.1016/j.yrtph.2021.105067>.
- Ag Seleci, D., G. Tsiliki, K. Werle, D. A. Elam, O. Okpowe, K. Seidel, X. Bi, et al. 2022. "Determining Nanoform Similarity via Assessment of Surface Reactivity by Abiotic and in Vitro Assays." *NanoImpact* 26: 100390. <https://doi.org/10.1016/j.impact.2022.100390>.
- Arts, J. H., M. Hadi, M. A. Irfan, A. M. Keene, R. Kreiling, D. Lyon, M. Maier, et al. 2015. "A Decision-Making Framework for the Grouping and Testing of Nanomaterials (DF4nanoGrouping)." *Regulatory Toxicology and Pharmacology: RTP* 71 (2 Suppl): S1–S27. <https://doi.org/10.1016/j.yrtph.2015.03.007>.
- Ayres, J. G., P. Borm, F. R. Cassee, V. Castranova, K. Donaldson, A. Ghio, R. M. Harrison, et al. 2008. "Evaluating the Toxicity of Airborne Particulate Matter and Nanoparticles by Measuring Oxidative Stress Potential—a Workshop Report and Consensus Statement." *Inhalation Toxicology* 20 (1): 75–99. <https://doi.org/10.1080/08958370701665517>.
- Bahl, A., B. Hellack, M. Wiemann, A. Giusti, K. Werle, A. Haase, and W. Wohlleben. 2020. "Nanomaterial Categorization by Surface Reactivity: A Case Study Comparing 35 Materials with Four Different Test Methods." *NanoImpact* 19: 100234. <https://doi.org/10.1016/j.impact.2020.100234>.
- Benzie, I. F., and J. J. Strain. 1996. "The Ferric Reducing Ability of Plasma (FRAP) as a Measure of "Antioxidant Power": the FRAP Assay." *Analytical Biochemistry* 239 (1): 70–76. <https://doi.org/10.1006/abio.1996.0292>.
- Boyles, M., F. Murphy, W. Mueller, W. Wohlleben, N. R. Jacobsen, H. Braakhuis, A. Giusti, and V. Stone. 2022. "Development of a Standard Operating Procedure for the DCFH2-DA Acellular Assessment of Reactive Oxygen Species Produced by Nanomaterials." *Toxicology Mechanisms and Methods* 32 (6): 439–452. <https://doi.org/10.1080/15376516.2022.2029656>.
- Braakhuis, H. M., F. Murphy, L. Ma-Hock, S. Dekkers, J. Keller, A. G. Oomen, and V. Stone. 2021. "An Integrated Approach to Testing and Assessment to Support Grouping and Read-Across of Nanomaterials after Inhalation Exposure." *Applied in Vitro Toxicology* 7 (3): 112–128. <https://doi.org/10.1089/avt.2021.0009>.
- Busquet, F., R. Strecker, J. M. Rawlings, S. E. Belanger, T. Braunbeck, G. J. Carr, P. Ceniin, et al. 2014. "OECD Validation Study to Assess Intra- and Inter-Laboratory Reproducibility of the Zebrafish Embryo Toxicity Test for Acute Aquatic Toxicity Testing." *Regulatory Toxicology and Pharmacology: RTP* 69 (3): 496–511. <https://doi.org/10.1016/j.yrtph.2014.05.018>.
- Caldeira, C., I. Garmendia Aguirre, D. Tosches, L. Mancini, E. Abbate, R. Farcal, D. Lipsa, et al. 2023. *Safe and Sustainable by Design Chemicals and Materials. Application of the SSbD Framework to Case Studies*. Luxembourg: Publications Office of the European Union.
- Dekkers, S., A. G. Oomen, E. A. Bleeker, R. J. Vandebriel, C. Micheletti, J. Cabellos, G. Janer, et al. 2016. "Towards a Nanospecific Approach for Risk Assessment." *Regulatory Toxicology and Pharmacology: RTP* 80: 46–59. <https://doi.org/10.1016/j.yrtph.2016.05.037>.
- Dekkers, S., S. W. P. Wijnhoven, H. M. Braakhuis, L. G. Soeteman-Hernandez, AJaM Sips, I. Tavernaro, A. Kraegeloh, and C. W. Noorlander. 2020. "Safe-by-Design Part I: Proposal for Nanospecific Human Health Safety Aspects Needed along the Innovation Process." *NanoImpact* 18: 100227. <https://doi.org/10.1016/j.impact.2020.100227>.
- Di Battista, V., C. Ribalta, K. Vilsmeier, D. Singh, P. Demokritou, E. Günther, K. A. Jensen, S. Dekkers, V. Adam, and W. Wohlleben. 2024a. "A Screening Approach to the Safe-and-Sustainable-by-Design Development of Advanced Insulation Materials." *Small (Weinheim an Der Bergstrasse, Germany)* 20 (32): e2311155. <https://doi.org/10.1002/sml.202311155>.
- Di Battista, V., K. R. Sanchez-Lievanos, N. Jeliakova, F. Murphy, G. Tsiliki, A. Zabeo, A. Gajewicz-Skretna, et al. 2024b. "Similarity of Multicomponent Nanomaterials in a Safer-by-Design Context: The Case of Core–Shell Quantum Dots." *Environmental Science: Nano* 11 (3): 924–941. <https://doi.org/10.1039/D3EN00338H>.
- Di Cristo, L., A. G. Oomen, S. Dekkers, C. Moore, W. Rocchia, F. Murphy, H. J. Johnston, et al. 2021. "Grouping Hypotheses and an Integrated Approach to Testing and Assessment of Nanomaterials following Oral Ingestion." *Nanomaterials* 11 (10): 2623. <https://doi.org/10.3390/nano11102623>.
- EC. 2019. *Communication from the Commission to the European Parliament, the Council, the European Economic and Social Committee and the Committee of the Regions: The European Green Deal*. European Commission, Brussels, COM(2019) 640.
- EC. 2020. *Chemicals Strategy for Sustainability towards a Toxic-Free Environment*. European Commission, Brussels, COM(2020) 667.
- Gandon, A., K. Werle, N. Neubauer, and W. Wohlleben. 2017. "Surface Reactivity Measurements as Required for Grouping and Read-across: An Advanced FRAS Protocol." *Journal of Physics: Conference Series* 838: 012033.
- Guadagnini, R., B. Halamoda Kenzaoui, L. Walker, G. Pojana, Z. Magdolenova, D. Bilanicova, M. Saunders, et al. 2015. "Toxicity Screenings of Nanomaterials: Challenges Due to Interference with Assay Processes and Components of Classic In Vitro Tests." *Nanotoxicology* 9 (Suppl 1): 13–24. <https://doi.org/10.3109/17435390.2013.829590>.
- Gulumian, M., and F. R. Cassee. 2021. "Safe by Design (SbD) and Nanotechnology: A Much-Discussed Topic with a Prudence?" *Particle and Fibre Toxicology* 18 (1): 32. <https://doi.org/10.1186/s12989-021-00423-0>.
- Hellack, B., C. Nickel, C. Albrecht, T. J. Kuhlbusch, S. Boland, A. Baeza-Squiban, W. Wohlleben, and R. P. F. Schins. 2017. "Analytical Methods to Assess the Oxidative Potential of Nanoparticles: A Review." *Environmental Science: Nano* 4: 1920–1934.
- Hsieh, S. F., D. Bello, D. F. Schmidt, A. K. Pal, A. Stella, J. A. Isaacs, and E. J. Rogers. 2013. "Mapping the Biological Oxidative Damage of Engineered Nanomaterials." *Small (Weinheim an Der Bergstrasse, Germany)* 9 (9-10): 1853–1865. <https://doi.org/10.1002/sml.201201995>.
- ISO. 2017. *ISO/TS 18827:2017. Nanotechnologies—Electron Spin Resonance (ESR) as a Method for Measuring Reactive Oxygen Species (ROS) Generated by Metal Oxide Nanomaterials*. Geneva, Switzerland: ISO.
- Janer, G., R. Landsiedel, and W. Wohlleben. 2021. "Rationale and Decision Rules behind the ECETOC NanoApp to

- Support Registration of Sets of Similar Nanoforms within REACH." *Nanotoxicology* 15 (2): 145–166. <https://doi.org/10.1080/17435390.2020.1842933>.
- Møller, P., N. R. Jacobsen, J. K. Folkmann, P. H. Danielsen, L. Mikkelsen, J. G. Hemmingsen, L. K. Vesterdal, L. Forchhammer, H. Wallin, and S. Loft. 2010. "Role of Oxidative Damage in Toxicity of Particulates." *Free Radical Research* 44 (1): 1–46. <https://doi.org/10.3109/10715760903300691>.
- Møller, P., P. H. Danielsen, D. G. Karottki, K. Jantzen, M. Roursgaard, H. Klingberg, D. M. Jensen, et al. 2014. "Oxidative Stress and Inflammation Generated DNA Damage by Exposure to Air Pollution Particles." *Mutation Research. Reviews in Mutation Research* 762: 133–166. <https://doi.org/10.1016/j.mrrev.2014.09.001>.
- Nel, A., T. Xia, L. Mädler, and N. Li. 2006. "Toxic Potential of Materials at the Nanolevel." *Science (New York, N.Y.)* 311 (5761): 622–627. <https://doi.org/10.1126/science.1114397>.
- Pal, A. K., S.-F. Hsieh, M. Khatri, J. A. Isaacs, P. Demokritou, P. Gaines, D. F. Schmidt, E. J. Rogers, and D. Bello. 2014. "Screening for Oxidative Damage by Engineered Nanomaterials: A Comparative Evaluation of FRAS and DCFH." *Journal of Nanoparticle Research* 16 (2): 2167. <https://doi.org/10.1007/s11051-013-2167-3>.
- Pedersen, E., and K. Fant. 2018. *Guidance Document on Good In Vitro Method Practices (GIVIMP): Series on Testing and Assessment No. 286*. Paris:OECD Publishing. <https://doi.org/10.1787/9789264304796-en>
- Peijnenburg, W., E. Ruggiero, M. Boyles, F. Murphy, V. Stone, D. A. Elam, K. Werle, and W. Wohlleben. 2020. "A Method to Assess the Relevance of Nanomaterial Dissolution during Reactivity Testing." *Materials (Basel, Switzerland)* 13 (10): 2235. <https://doi.org/10.3390/ma13102235>.
- Piret, J. P., O. M. Bondarenko, M. S. P. Boyles, M. Himly, A. R. Ribeiro, F. Benetti, C. Smal, et al. 2017. "Pan-European Inter-Laboratory Studies on a Panel of in Vitro Cytotoxicity and Pro-Inflammation Assays for Nanoparticles." *Archives of Toxicology* 91 (6): 2315–2330. <https://doi.org/10.1007/s00204-016-1897-2>.
- Riebeling, C., M. Wiemann, J. Schneckeburger, TaJ Kuhlbusch, W. Wohlleben, A. Luch, and A. Haase. 2016. "A Redox Proteomics Approach to Investigate the Mode of Action of Nanomaterials." *Toxicology and Applied Pharmacology* 299: 24–29. <https://doi.org/10.1016/j.taap.2016.01.019>.
- Rogers, E. J., S. F. Hsieh, N. Organti, D. Schmidt, and D. Bello. 2008. "A High Throughput in Vitro Analytical Approach to Screen for Oxidative Stress Potential Exerted by Nanomaterials Using a Biologically Relevant Matrix: Human Blood Serum." *Toxicology in Vitro: An International Journal Published in Association with BIBRA* 22 (6): 1639–1647. <https://doi.org/10.1016/j.tiv.2008.06.001>.
- Ruijter, N., L. G. Soeteman-Hernández, M. Carrière, M. Boyles, P. McLean, J. Catalán, A. Katsumiti, et al. 2023. "The State of the Art and Challenges of In Vitro Methods for Human Hazard Assessment of Nanomaterials in the Context of Safe-by-Design." *Nanomaterials* 13 (3): 472. <https://doi.org/10.3390/nano13030472>.
- Song, B., T. Zhou, W. Yang, J. Liu, and L. Shao. 2016. "Contribution of Oxidative Stress to TiO<sub>2</sub> Nanoparticle-Induced Toxicity." *Environmental Toxicology and Pharmacology* 48: 130–140. <https://doi.org/10.1016/j.etap.2016.10.013>.
- Stone, V., S. Gottardo, EaJ Bleeker, H. Braakhuis, S. Dekkers, T. Fernandes, A. Haase, et al. 2020. "A Framework for Grouping and Read-across of Nanomaterials- Supporting Innovation and Risk Assessment." *Nano Today*. 35: 100941. <https://doi.org/10.1016/j.nantod.2020.100941>.